

Biomedical Applications of Intensity and Curvature Measures: The Case of Magnetic Resonance Imaging of the Human Brain

Carlo Ciulla, Ustijana Reckoska Shikoska, Dijana Capeska Bogatinoska
 University for Information Science & Technology
 “St. Paul the Apostle”
 Ohrid, Macedonia
 e-mail: carlo.ciulla@uist.edu.mk, cxc2728@njit.edu,
 ustijana@gmail.com, dijana.c.bogatinoska@uist.edu.mk

Filip A. Risteski, Dimitar Veljanovski
 Skopje City General Hospital
 Skopje, Macedonia
 e-mail: risteski@bolnica.org.mk,
 dveljanovski@bolnica.org.mk

Abstract—This paper intends to present a novel approach to the extraction of additional and/or complementary biomedical information from the Magnetic Resonance Imaging (MRI) of the human brain. The extraction of the biomedical information is conducted through three mathematical engineering tools called Classic-Curvature, Intensity-Curvature Functional and Intensity-Curvature Measure, which are calculated through a model function fitted to the MRI data. The mathematical engineering tools require that the model function benefits of the property of second-order differentiability. The Classic-Curvature, the Intensity-Curvature Functional and the Intensity-Curvature Measure descend from the unifying theory and the unified theory originally conceived for the improvement of the interpolation error. The advantage provided through the methodological approach is that an immense number of possible Classic-Curvature, Intensity-Curvature Functional and Intensity-Curvature Measure images can be derived through re-sampling at the intra-pixel coordinate, and this fact provides the possibility to choose images which give the best result in diagnostic practice. The biomedical information might be used in telemedicine.

Keywords—Model Function; Classic-Curvature; Intensity-Curvature Functional; Signal-Image; Magnetic Resonance Imaging (MRI); Human Brain.

I. INTRODUCTION

The introduction section will describe the proposal, it will also describe why the theoretical basis of the present work differs from the state of the art and also it will outline the contribution of this paper.

A. Description of the Approach

Let us define the grid node as the location where sampling occurs in either one dimension (1D), two dimensions (2D), or three dimensions (3D). In a sequel of digital samples, in either 1D, 2D or 3D, let a given intra-node location be called the re-sampling location. The problem statement is given hereto: the calculation of three continuous math formulae from a discontinuous domain created by a sequel of digital samples. The requirement of the solution to the problem is that a model function, which embeds the property of second-order differentiability [1], needs to be fitted to the discontinuous domain.

The solution to the herein stated problem consists in the calculation of the Classic-Curvature at the re-sampling location [1]. Specifically, given an image and fitting the model function to the image, it is possible to calculate the Classic-Curvature through the summation of all of the partial second order derivatives of the Hessian [1] of the model function [1]. The partial second order derivatives are calculated at the re-sampling location. The re-sampling location is the intra-pixel coordinate where the signal-image is calculated through the model function.

The calculation of the Classic-Curvature makes it possible also to calculate the Intensity-Curvature Functional [2][3] at the re-sampling location as follows. The ratio between two terms: (i) the integral of the product between the signal intensity and the Classic-Curvature both of them calculated at the grid node; and (ii) the integral of the product between the signal intensity and the Classic-Curvature both of them calculated at the re-sampling location. The calculation of the Intensity-Curvature Measure has been introduced in [4].

B. Comparison with other Solutions

The literature shows a widespread use of approximations of the curvature of the signal-image through compact finite differences, and/or gradients and/or the Sobel operator [5] for the calculation of the first order derivative of the signal-image see, for instance, the work reported in [5]-[8]. The necessity of having a rigorous method, which is based on calculus, in order to quantify the curvature of the signal-image, makes the present paper different and unique in the field of biomedical signal-image processing. In fact, in this work, the calculation of the Classic-Curvature is made through all of the second-order partial derivatives of the Hessian of the model polynomial function fitted to the MRI data. The advantage is that of summing up all of the partial second order derivatives of the Hessian of the model function fitted to the image. By doing so, the covariates partial derivatives are included in the calculation of the Classic-Curvature, the Intensity-Curvature Functional and the Intensity-Curvature Measure.

C. Applicability to the Life Sciences

The proposal presented in this paper has the potential to contribute to life sciences because of the three novel images: Classic-Curvature, Intensity-Curvature Functional (see

Figure 1) and Intensity-Curvature Measure (see Figures 9 and 10), which embeds biomedical information content having diagnostic value. For example, in human brain imaging, for what pertains to: (i) the demarcation of anatomical structures, (ii) highlighting of the difference between gray and white matter; both in normal and in pathological biomedical images, and (iii) the extraction of additional and/or complementary information from pathological MRI. The connection between the research here presented and the Information Communication Technologies is in the field of Telemedicine. Figure 1 shows the Original MRI in (a), which is provided by the courtesy of OASIS database [9]-[14][15]. Figure 1b shows the Classic-Curvature of the MRI seen in (a). Figure 1c shows the Intensity-Curvature Functional of the MRI seen in (a). The image in Figure 1b is calculated with the two-dimensional Lagrange polynomial [3] when re-sampling of the misplacement of 0.1mm along both of x and y axis, whereas the image in Figure 1c is calculated with the bivariate linear function [16], when re-sampling of the misplacement of 0.01mm along the x axis and 0.01mm along the y axis. In Figure 1, the image in (c) shows a third dimension perpendicular to the imaging plane along with the difference between gray and white matter. Both of the images in (b) and (c) are contrast-brightness enhanced.

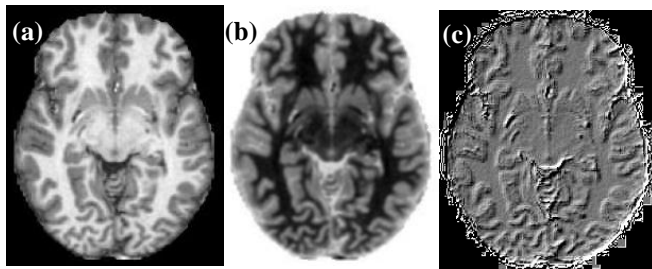


Figure 1. The image in (a) shows the original MRI and comprises of a 205x246 pixels matrix with 1.00mm x 1.00mm pixel size; (b) shows the Classic-Curvature of (a), which marks a clear difference between gray and white matter of the human brain and (c) shows the Intensity-Curvature Functional of (a).

In this paper, emphasis is given to four model functions, specifically: (i) the bivariate quadratic B-Spline polynomial [3], (ii) the bivariate cubic Lagrange polynomial [3], (iii) the one-dimensional Sinc function [2], and (iv) the bivariate linear function [16]. It is evident that the aforementioned four model functions are capable, through the application of the Classic-Curvature, the Intensity-Curvature Functional and the Intensity-Curvature Measure, to extract information from the MRI images, which is not readily observable into the original images.

Section II will focus on the capability of the Classic-Curvature, the Intensity-Curvature Functional and the Intensity-Curvature Measure to perform feature extraction from the original image. In Section III, the practical implications of this work will be addressed placing the emphasis on the methodological approach and also on the

value added to the original MRI through the use of the three mathematical engineering tools used in this piece of research. Finally, Section IV concludes the paper.

II. RESULTS

This section presents qualitative results obtained through fitting to the MRI data of the human brain: (i) the bivariate quadratic B-Spline, (ii) the cubic Lagrange polynomial, and also (iii) the one-dimensional Sinc interpolation function [2]. Figure 2 shows two of the MRI images employed in this piece of research, which are referred here as to be the original MRI. Some of the Classic-Curvature and the Intensity-Curvature Functional reported in this section have been calculated on the basis of the images shown in Figure 2. The MRI image shown in Figure 2a is provided by the courtesy of Casa di Cure Triolo - Zanca, Palermo - Italy [3]. The MRI image shown in Figure 2b is provided by the courtesy of the OASIS database [15]. In Figure 2, the image in (a) has been scaled to enhance the visual appearance of the picture.

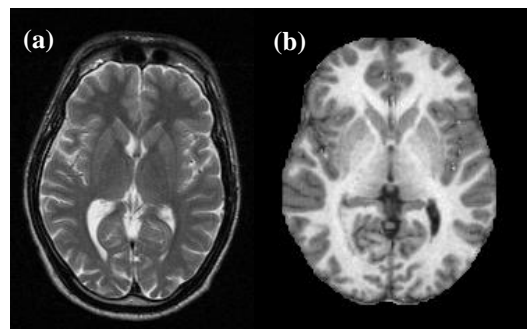


Figure 2. Original Magnetic Resonance Imaging data: (a) the image is made of a 176 x 234 pixels matrix with pixel size of 1mm x 1mm; (b) the image is made of a 176 x 208 pixels matrix with pixel size of 1mm x 1mm.

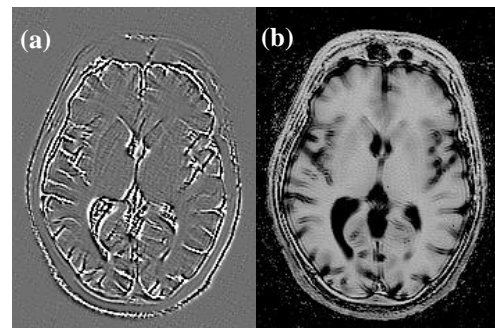


Figure 3. The image in (a) shows the Classic-Curvature and the image in (b) shows the Intensity-Curvature Functional. The brain structures highlighted in (a) are those of the sulci and the brain ventricles (see white contours). In (b) the emphasis is still on the sulci of the human brain and the depth is highlighted.

Figure 3 shows the Classic-Curvature image in (a) and the Intensity-Curvature Functional image in (b). Specifically, since it is the objective of this piece of research to assess the capability of two of the mathematical engineering tools to provide complementary information

through feature extraction from the original MRI, the reader should compare the appearance of the Classic-Curvature and the Intensity-Curvature Functional images with the original MRIs shown in Figure 2. Both of the images in Figure 3 were obtained when fitting to the signal-data the bivariate quadratic B-Spline re-sampling of 0.01mm along the x direction and 0.01mm along the y direction. Both of the images in Figure 3 are contrast-brightness enhanced. Figure 4 shows two Intensity-Curvature Functional images obtained when fitting the bivariate quadratic B-Spline to the human brain data and when re-sampling was performed at the misplacement $(x, y) \equiv (0.01\text{mm}, 0.001\text{mm})$ with the value of the 'a' constant parameter set to 7 in both of (a) and (b). The difference observable between (a) and (b) is attributable to the pre-processing step, which standardizes (see (a)), and scales (see (b)) the pixel intensity respectively.

In Figure 4, the image in (a) shows a neat distinction between the gray and the white matter of the human brain, whereas the image in (b) shows the same distinction however with a third dimension visible in the direction perpendicular to the image plane. Both of the images are contrast-brightness enhanced.

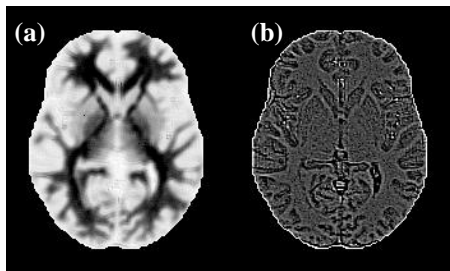


Figure 4. The images in (a) and (b) are both Intensity-Curvature Functional of the original MRI shown in Figure 2b and they were obtained when fitting the bivariate quadratic B-Spline to the signal data.

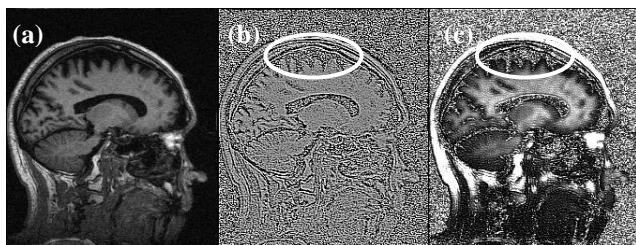


Figure 5. The image in (a) is the original MRI and the images in (b) and (c) are Intensity-Curvature Functional with visible and well demarcated brain anatomical structures.

Figure 5 shows two Intensity-Curvature Functional images in (b) and in (c) obtained from the original MRI shown in (a). The original MRI is provided by the courtesy of the OASIS database and was collected on a subject classified positive to the Clinical Dementia Rating (CDR) [10][12]. In Figure 5, the pixels matrix size is 256 x 256 with pixel size 1mm x 1mm. The Intensity-Curvature Functional images were obtained when fitting the bivariate quadratic B-Spline

to the signal-image, specifically when using the 'a' constant parameter set to 3.54 (b) and -3.54 (c). The misplacement used for re-sampling is $(x, y) \equiv (0.01\text{mm}, 0.01\text{mm})$ in both of (b) and (c). What is remarkable in Figure 5 is the fact that the shrinkage of the human cortex, which is well visible in (a), is also visible in (b) and (c) where the value of the Intensity-Curvature Functional is comparable to the noise level of the rest of the image (see inside the white ellipses).

In Figure 5, the human cortex is distinguishable in both images (b) and (c). The images were cropped to highlight the regions of interest and they are contrast-brightness enhanced.

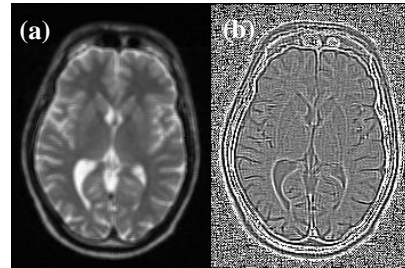


Figure 6. The image in (a) shows the Classic-Curvature and the image in (b) shows the Intensity-Curvature Functional. The two images were obtained when re-sampling with the bivariate cubic Lagrange polynomial with a misplacement of $(x, y) \equiv (0.01\text{mm}, 0.01\text{mm})$ in (a) and a misplacement of $(x, y) \equiv (0.95\text{mm}, 0.95\text{mm})$ in (b).

Figure 6 shows results obtained when fitting the bivariate cubic Lagrange polynomial to the brain image data. While the Classic-Curvature demonstrates faithful reproduction of the original MRI therefore showing all of the human brain features, the Intensity-Curvature Functional places the emphasis on the small features of the human brain such as the sulci showing well demarcated anatomy. The same can be said for the brain ventricles. In other words, the image depicted in (b) performs feature extraction from the image seen in (a), therefore showing details that are not readily seen in (a), neither in the original MRI. A similar behavior of both the Classic-Curvature and the Intensity-Curvature Functional was already observed in Figure 3. In Figure 6, likewise indicated in Figure 2, the images comprise of a 176 x 234 pixels matrix with pixel size of 1mm x 1mm and they are contrast-brightness enhanced.

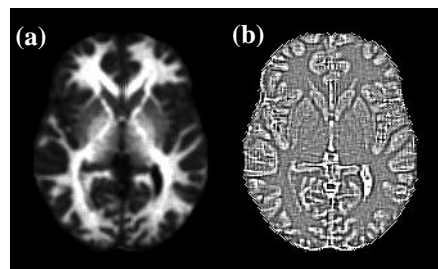


Figure 7. The image in (a) shows the Classic-Curvature and the image in (b) shows the Intensity-Curvature Functional. The original MRI is provided by the courtesy of the OASIS database [15].

Figure 7 shows the Classic-Curvature in (a) and the Intensity-Curvature Functional in (b). The images were obtained when fitting the bivariate cubic Lagrange polynomial and re-sampling with a misplacement $(x, y) \equiv (0.01\text{mm}, 0.01\text{mm})$ in (a) and a misplacement $(x, y) \equiv (0.95\text{mm}, 0.95\text{mm})$ in (b). The behavior of the two mathematical engineering tools is similar to the one showed in Figure 6. The Classic-Curvature of Figure 7a shows remarkable reproduction of the original MRI image features overall all of the anatomical structures. The Intensity-Curvature Functional seen in Figure 7b performs feature extraction, showing details of the MRI, which are not visible otherwise. And specifically, in both of (a) and (b) is highlighted the distinction between gray and white matter of the human brain. Figure 7b shows similarities with Figure 4b (also an Intensity-Curvature Functional image), with the exception that the third dimension seen as perpendicular to the image plane is not visible in Figure 7b. However, the level of details is more pronounced in Figure 7b than it is in Figure 4b, notwithstanding the contrast enhancement of the two images. Likewise the images in Figure 4, the images in Figure 7 have a pixels matrix size of 176×208 with pixel size of $1\text{mm} \times 1\text{mm}$. In Figure 7, the images in (a) and (b) are contrast-brightness enhanced.

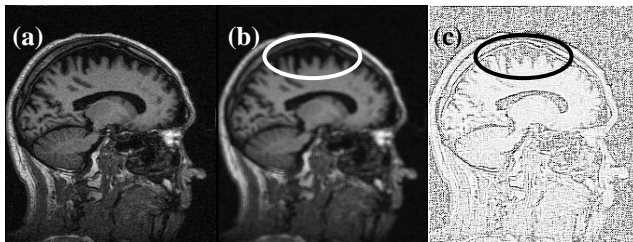


Figure 8. The image in (a) shows the original MRI, and (b) and (c) show the Classic-Curvature and the Intensity-Curvature Functional respectively. The effect of the Intensity-Curvature Functional is not as accentuated as the one seen in Figure 5c, and it is similar to the effect seen in Figure 5b.

Figure 8 shows the Classic-Curvature (see (b)) and the Intensity-Curvature Functional (see (c)) of the pathological MRI shown in (a). The subject was classified positive to the Clinical Dementia Rating (CDR) [10][12]. The Classic-Curvature image reproduces the original MRI shown in (a) with high level of details for what pertains to all of the anatomical structures and therefore highlights the shrinkage of cortical surface that can be seen in the regions inside the white ellipse in (b). As far as regards to the shrinkage of the cortical surface, the Intensity-Curvature Functional image seen in (c) shows that the intensity level is comparable to the noise level (see regions inside the black ellipse in (c)), thus adding confirmation to the observation made through the Classic-Curvature image. Both of the Classic-Curvature and the Intensity-Curvature Functional were obtained when fitting the bivariate cubic Lagrange polynomial and re-sampling of a misplacement $(x, y) \equiv (0.01\text{mm}, 0.01\text{mm})$. The pixels matrix size is 256×256 with pixel size $1\text{mm} \times$

1mm . The images were cropped to highlight the regions of interest and were contrast-brightness enhanced.

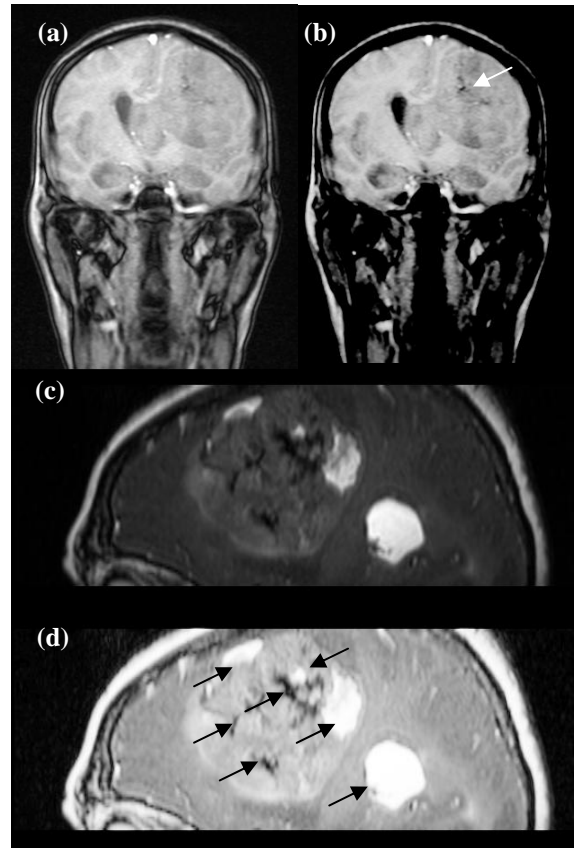


Figure 9. The images in (a) (contrast-brightness enhanced) and in (c) show the original MRI. The images in (b) and in (d) show the Intensity-Curvature Measure obtained fitting the data with the one-dimensional Sinc interpolation function.

Figure 9 shows in (a) and in (c) the original MRI with the tumor. Also, Figure 9 shows in (b) and in (d) the Intensity-Curvature Measure [1] obtained with the one-dimensional Sinc function. The interesting feature of the Intensity-Curvature Measure (see (b)) is the capability to highlight the tumor when extracting information from the original MRI seen in (a). Changing the brightness-contrast enhancement of Figure 9b yields an image, which is clearer than the one shown in (a), and which is the highlight of the tumor in its full spatial extent. The comparison between Figure 9a and 9b makes a clear and direct point, which is that the behavior of the mathematical engineering images is capable to add additional information to the original MRI (see Figure 9b: clearer contour line of the tumor and the dark spot indicated by the white arrow, which is presumably blood). In Figure 9b (contrast-brightness enhanced), the Intensity-Curvature Measure shows the capability to reveal the tumor with a perspective, which is different from the original image seen in Figure 9a. The tumor region is more clearly demarcated in (b) than it is in (a), whereas Figure 9d (contrast-brightness enhanced) demonstrates the capability of the

Intensity-Curvature Measure to focus on the fluids of the tumor as it is indicated through the arrows. The matrix size in Figures 9a and 9b is 512x512 pixels with 0.55mm x 0.55mm pixel size. The matrix size in Figures 9c and 9d is 512x512 pixels with 0.39mm x 0.39mm pixel size. The images in Figures 9a, 9b, 9c and 9d were cropped so to focus on the regions of interest. Similar behavior is observable in the mathematical engineering images shown by this piece of research. Figure 9d shows the contour line of the tumor and the fluids such as water and blood (see arrows). Both of the images seen in Figures 9b and 9d where obtained when re-sampling of 0.1mm along the x axis alone. The lesson learned is that the three mathematical engineering tools are able to extract additional and/or complementary information from MRI images. Future work should address the biomedical value of the information extracted from the MRI images through the methodology presented in this paper.

III. DISCUSSION

This Section discusses on the effect of the contrast-brightness enhancement and also offers insights about the contribution of the works herein presented to the biomedical imaging processing literature stressing on the use of the mathematical engineering tools used to extract complementary and/or additional information from Magnetic Resonance Images of the human brain.

A. The Effect of the Brightness-Contrast Enhancement

The mathematical engineering images resulting from the original MRI: (i) Classic-Curvature, (ii) Intensity-Curvature Functional and (iii) Intensity-Curvature Measure have been object of brightness-contrast enhancement, whereas the original MRI brain images were not object of brightness-contrast enhancement (except for Figure 9a).

It can be argued that using the aforementioned enhancement in both the original MRI and the mathematical engineering images yields the same (or similar) result and thus the mathematical engineering images are not capable to add additional information to the original MRI (such possibility is explored in Figure 10). However, the capability of the mathematical engineering images of adding additional and/or complementary is supported in: (i) Figures 3, 4, 7 and 9b, and (ii) the following facts.

The first fact is that the mathematical engineering images, as widely observed in both of the cases herein reported and the cases that were reported elsewhere [1][3][17], present the characteristic of having pixel intensity values, which is quite different from the original brain images. Even with the large difference in pixel intensity values it is possible to set the same level of brightness-contrast enhancement for both of the original MRI and the mathematical engineering images. However, when the level of brightness-contrast enhancement is set the same, in the vast majority of the cases, different demarcation and appearance of the overall anatomical

structure of the brain images was observed (see Figure 9a versus Figure 9b). Also, the aforementioned pixel intensity value difference makes it necessary the brightness-contrast enhancement of the mathematical engineering images so to view the content.

The second fact is consequential to the first one and is that the brightness-contrast enhancement is necessary to highlight the content of the mathematical engineering images so to reveal the additional and/or complementary information to the MRI. Indeed, through the mathematical engineering images it is possible to see: (i) the depth of the brain sulci (see Figure 3), (ii) the anatomical structure (see Figure 6a), (iii) the difference between gray and white matter (see Figure 1b and Figure 3a), (iv) the presence of fluids such as blood and water (see Figure 9d: the pathological image) and also the third dimension (see Figure 1c).

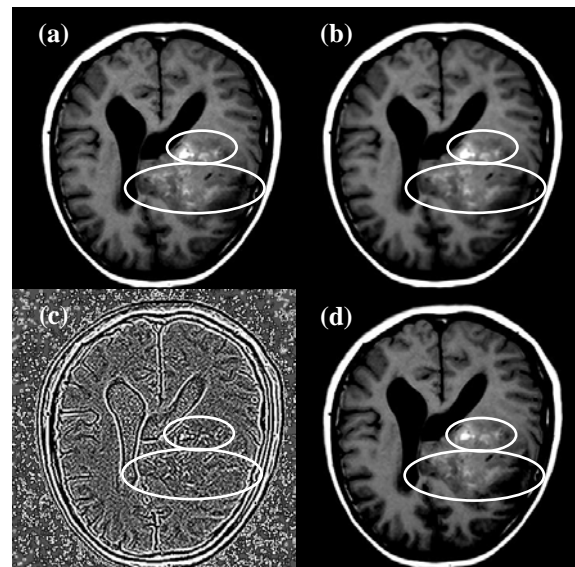


Figure 10. The image in (a) shows the original MRI with a tumor, whereas (b) shows the Classic-Curvature image, (c) shows the Intensity-Curvature Functional, and (d) shows the Intensity-Curvature Measure.

In order to investigate what happens when the contrast-brightness enhancement is set the same for both of the mathematical engineering images and the original MRI the following experiment was performed. Figure 10 reports the results of the experiment, which show that the Classic-Curvature (see Figure 10b) and the Intensity-Curvature Measure (see Figure 10d) images present almost the same characteristics of the original MRI, except for some blurring, which is visible because of the mathematical processing. Instead, the Intensity-Curvature Functional (see Figure 10c) shows details that are not observable in the original MRI (see inside the white ellipses). The images in Figure 10b and Figure 10c were obtained when fitting to the MRI data the bivariate cubic Lagrange model function when re-sampling of 0.1mm along both x and y directions, whereas the image in Figure 10d was obtained when fitting

the one-dimensional Sinc model function when re-sampling of 0.1mm along the x direction. The matrix size of the images in Figure 10 is 512x512 with pixel size of 0.49 mm x 0.49 mm. The images in (a), (b) and (d), have been set to the same brightness-contrast adjustment. In (d) the Intensity-Curvature Functional shows a complementary perspective to the images seen in (a) and (b), highlighting the structure of the tumor fluids such as blood and water. The images were cropped to highlight the regions of interest and are all contrast-brightness enhanced.

The significance of Figure 10 is that the mathematical engineering images are capable to show the anatomical structure of the human brain likewise the original MRI does. This fact is positive to the research question of the herein presented work, which investigates whether the mathematical engineering images add complementary information to the MRI. Also, Figure 10c shows that the Intensity-Curvature Functional presents details which are not visible in the original MRI. Such fact is in favor to the aforementioned research question. Hence, the contrast-brightness enhancement, is not a confounding factor, it is indeed a requirement for the extraction of additional and/or complementary information from the MRI of the human brain because at the least the mathematical engineering images can reproduce the same level of details of the MRI of the human brain (see Figure 10).

B. The Contribution to Biomedical Image Processing

A well-defined novel formulation of three specific mathematical engineering instruments has been conceived [2]-[4]. The novel formulation provides the solution of the biomedical signal processing problem, which consists in extracting additional information from the Magnetic Resonance Imaging (MRI) signal of the human brain.

The three mathematical engineering instruments are called: (i) Classic-Curvature, (ii) Intensity-Curvature Functional and (iii) Intensity-Curvature Measure. The three math instruments make use of the second order derivatives of the model function fitted to the data. The aforementioned instruments makes it possible to re-image the Magnetic Resonance Imaging (MRI) image data of the human brain into three novel domains where there exists features that would not be otherwise observable in the original MRI images.

The research herein presented has significance in the field of biomedical signal processing and more generally in diagnostic radiology because brings to the attention of the reader the existence of three novel domains. The novel domains have been revealed through the use of conceptual forms descending from one main signal processing technique, which is that of the calculation of the Classic-Curvature [1]-[3]. In fact, the calculation of the Classic-Curvature enables also the calculation of the Intensity Curvature Functional and the Intensity-Curvature Measure. The work herein presented demonstrates the feasibility of the calculation of the Classic-Curvature, the Intensity-Curvature Functional and the Intensity-Curvature Measure from the two-dimensional MRI of the human brain both in normal and

pathological cases. The calculation of the Intensity-Curvature Functional in three dimensions is also possible [17].

IV. CONCLUSION

This paper considered the problem of the three mathematical engineering tools that are used to provide useful information, which is not readily observable into the original MRI images. This research also provides results which evaluate the performance of the proposed mathematical engineering tools. The results show that the Classic-Curvature image reproduces the original MRI image with high level of details and both of the Intensity-Curvature Functional and the Intensity-Curvature Measure performs feature extraction showing details of the MRI which are not visible otherwise. The advantage provided through the re-sampling process is indeed a fact which gives an immense number of possible Classic-Curvature, Intensity-Curvature Functional and Intensity-Curvature Measure images. Also, it provides the freedom to choose images which give best result in diagnostic practice. The mathematical models rely on software code implementing complex math formulas. Due to the originality of the research here presented it is not possible to compare our results with previous research findings. However, since we provide the software free of charge, the mathematical engineering tools are easily available to the scientific community.

ACKNOWLEDGMENT

Hereto reporting findings that benefit from OASIS data [16], we are due to mention the following grant numbers: P50 AG05681, P01 AG03991, R01 AG021910, P50 MH071616, U24 RR021382 R01 MH56584 [16]. The MRI images shown in Figure 1a (© IGI Global Publisher) and Figure 2b (© IGI Global Publisher) are reprinted from [2]. The MRI image shown in Figure 2a (© Carlo Ciulla) is reprinted from [3].

REFERENCES

- [1] C. Ciulla, "On the calculation of the signal-image classic-curvature: A second order derivatives based approach", *International Journal of Emerging Trends & Technology in Computer Science (IJETTCS)*, vol. 2, no. 4, 2013, pp. 158-165.
- [2] C. Ciulla, "Improved signal and image interpolation in biomedical applications: The case of magnetic resonance imaging (MRI)", *Medical Information Science Reference - IGI Global Publisher, Hershey, PA, U.S.A., 2009.*
- [3] C. Ciulla, "Signal resilient to interpolation: An exploration on the approximation properties of the mathematical functions", *CreateSpace Publisher, U.S.A., 2012.*
- [4] C. Ciulla, "On the signal-image intensity-curvature content", *International Journal of Image, Graphics and Signal Processing*, vol. 5, no. 5, 2013, pp. 15-21.
- [5] Y. Cha and S. Kim, "The error-amended sharp edge (EASE) scheme for image zooming", *IEEE Transactions on Image Processing*, vol. 16, no. 6, 2007, pp. 1496-1505.

- [6] J. Prewitt, "Object enhancement and extraction", In: Picture Processing and Psychopictorics, B. Lipkin and A. Rosenfeld, Eds. New York: Academic, 1970, pp. 75-149.
- [7] S.K. Lele, "Compact difference schemes with spectral-like resolution", *Journal of Computational Physics*, vol. 103, 1992, pp. 16-42.
- [8] H. Farid and E.P. Simoncelli, "Differentiation of discrete multidimensional signals", *IEEE Transactions on Image Processing*, vol. 13, no. 4, 2004, pp. 496-508.
- [9] R.L. Buckner et al., "A unified approach for morphometric and functional data analysis in young, old, and demented adults using automated atlas-based head size normalization: Reliability and validation against manual measurement of total intracranial volume", *Neuroimage*, vol. 23, no. 2, 2004, pp. 724-738.
- [10] A. F. Fotenos, A. Z. Snyder, L. E. Girton, J. C. Morris, and R. L. Buckner, "Normative estimates of cross-sectional and longitudinal brain volume decline in aging and AD", *Neurology*, vol. 64, 2005, pp. 1032-1039.
- [11] D. S. Marcus et al., "Open access series of imaging studies (OASIS): Cross-sectional MRI data in young, middle aged, nondemented, and demented older adults", *Journal of Cognitive Neuroscience*, vol. 19, no. 9, 2007, pp. 1498-1507.
- [12] J. C. Morris, "The clinical dementia rating (CDR): current version and scoring rules", *Neurology*, vol. 43, no. 11, 1993, pp. 2412b-2414b.
- [13] E. H. Rubin et al., "A prospective study of cognitive function and onset of dementia in cognitively healthy elders", *Archives of Neurology*, vol. 55, no. 3, 1998, 2001, pp. 395-401.
- [14] Y., Zhang, M. Brady, and S. Smith, "Segmentation of brain MR images through a hidden Markov random field model and the expectation maximization algorithm", *IEEE Transactions on Medical Imaging*, vol. 20, no. 1, 2001, pp. 45-57.
- [15] OASIS database <<http://www.oasis-brains.org/>> 2014.05.15
- [16] C. Ciulla and F. P. Deek "The Sub-Pixel Efficacy Region of the Bivariate Linear Interpolation Function", *International Journal of Computer Applications in Technology*, vol. 49, nos. 3/4, May, 2014, pp.270–281.
- [17] C. Ciulla, "The intensity-curvature functional of the trivariate cubic Lagrange interpolation formula", *International Journal of Image, Graphics and Signal Processing*, vol. 5, no. 10, 2013, pp. 36-44.